Inorg. Chem. **2008**, *47*, 2601−2607

Convenient Route Leading to Neutral *fac*-M(CO)$_3$(NNO) Complexes (M = Re, ^{99m}Tc) Coupled to Amine Pharmacophores

Aris Chiotellis,[†] Charalambos Tsoukalas,[†] Maria Pelecanou,[‡] Catherine Raptopoulou,[§] Aris Terzis,[§] Minas Papadopoulos,[†] Zetta Papadopoulou-Daifoti,[⊥] and Ioannis Pirmettis*[,†]

Institute of Radioisotopes−Radiodiagnostic Products, National Centre for Scientific Research "Demokritos", 15310 Athens, Greece, Institute of Biology, National Centre for Scientific Research "Demokritos", 15310 Athens, Greece, Institute of Materials Science, National Centre for Scientific Research "Demokritos", 15310 Athens, Greece, Department of Pharmacology, Medical School, University of Athens, 11527 Athens, Greece

Received September 28, 2007

The synthesis and characterization of three neutral tricarbonyl *fac*-M(CO)$_3$(NNO) (M = Re, ^{99m}Tc) complexes based on the picolylamine *N,N*-diacetic acid (PADA) ligand is reported. One of the two carboxylate groups of the PADA ligand is efficiently and conveniently derivatized with an amine nucleophile through the use of the PADA anhydride. In this work, aniline, benzylamine and pyrrolidine were used as model amine nucleophiles. The rhenium complexes were synthesized using the [NEt$_4$]$_2$[Re(CO)$_3$Br$_3$] precursor and fully characterized by elemental analysis, spectroscopic methods, and X-ray crystallography. The analogous technetium-99m complexes were also prepared quantitatively using the [^{99m}Tc(CO)$_3$(H$_2$O)$_3$]$^+$ precursor. The reaction scheme presented for the synthesis of the *fac*-M(CO)$_3$(NNO) (M = Re, ^{99m}Tc) complexes can be applied to the development of target-specific radiopharmaceuticals because, in principle, any bioactive pharmacophore bearing an amine group can be used in the place of the model amine nucleophiles.

Introduction

The coordination chemistry of technetium and its surrogate rhenium is the focus of intense research activity mainly due to the extensive use of the radioactive isotopes of these elements in nuclear medicine. Technetium-99m ($t_{1/2}$ = 6 h, E_γ = 140 KeV) is the radioisotope of choice for nuclear medical imaging, due to its ideal nuclear properties, its low cost, and widespread availability[1] while rhenium-188 ($t_{1/2}$ = 0.7 d, E_{max} = 2.12 MeV) finds growing application in radiation therapy.[2] Both isotopes are readily available as permetallates M(VII)O$_4^-$ from a ^{99}Mo/^{99m}Tc or ^{188}W/^{188}Re generator system, respectively. New metal cores and ligand systems are continuously emerging in the literature aiming at complexes with high in vivo stability, favorable pharmacokinetic properties and target tissue specificity.[3] The recent introduction of the air-stable *fac*-[M(CO)$_3$(H$_2$O)$_3$]$^+$ (M = Tc or Re) synthon produced by the gentle reduction of M(VII) to M(I) under 1 atm of CO, established the M(I)(CO)$_3^+$ core as an easily accessible platform in the search for new radiopharmaceuticals.[4] The three aqua ligands of the *fac*-[M(CO)$_3$(H$_2$O)$_3$]$^+$ synthon are labile and readily substituted by a variety of functional groups including amines, thioethers, imines, thiols, and phosphines to give stable hexacoordinated complexes.[5] Furthermore,

* Corresponding author: Tel.: + 30210 6503921. Fax: + 30210 6524 480. E-mail: ipirme@ rrp.demokritos.gr.

[†] Institute of Radioisotopes−Radiodiagnostic Products, National Centre for Scientific Research "Demokritos".

[‡] Institute of Biology, National Centre for Scientific Research "Demokritos".

[§] Institute of Materials Science, National Centre for Scientific Research "Demokritos".

[⊥] University of Athens.

(1) (a) Jurisson, S.; Berning, D.; Wei, J.; Ma, D. *Chem. Rev.* **1993**, *93*, 1137–1156. (b) Dilworth, J. R.; Parrott, S. J. *Chem. Soc. Rev.* **1998**, *27*, 43–55. (c) Jurisson, S. S.; Lydon, J. D. *Chem. Rev.* **1999**, *99*, 2205–2218. (d) Liu, S.; Edwards, D. S. *Chem. Rev.* **1999**, *99*, 2235–2268.

(2) (a) Volkert, W. A.; Hoffman, T. J. *Chem. Rev.* **1999**, *99*, 2269–2292. (b) Schubiger, P. A.; Alberto, R.; Smith, A. *Bioconjugate Chem.* **1996**, *7*, 165–179.

(3) Banerjee, S. R.; Maresca, K. P.; Francesconi, L.; Valliant, J.; Babich, J. W.; Zubieta, J. *Nucl. Med. Biol.* **2005**, *32*, 1–20.

(4) (a) Alberto, R.; Schibli, R.; Egli, A.; Schubiger, A. P. *J. Am. Chem. Soc.* **1998**, *120*, 7987–7988. (b) Alberto, R. *Top. Curr. Chem.* **2005**, *252*, 1–44.

10.1021/ic7019268 CCC: $40.75
Published on Web 02/23/2008

Scheme 1

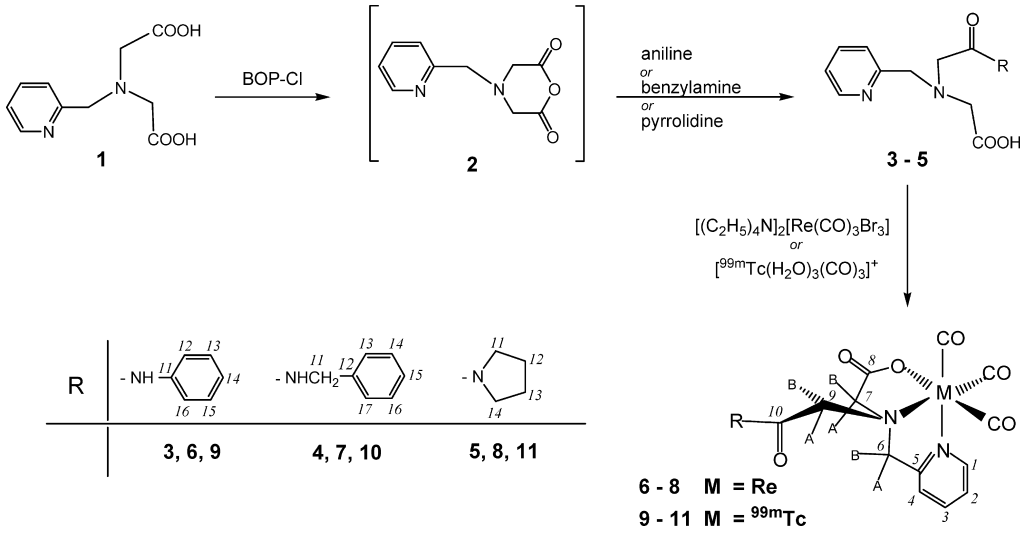

the small size and kinetic inertness of the $M(I)(CO)_3^+$ core make it suitable for the labeling of biologically active molecules with minimum disruption of their activity or specificity.

The picolylamine *N*,*N*-diacetic acid ligand, PADA, (**1**, Scheme 1) has been frequently employed in the literature as a ligand for the *fac*-$M(I)(CO)_3^+$ (M = Re or ^{99m}Tc) core in the synthesis of target-specific complexes due to its favorable properties.[3,6,7] Specifically, PADA is a tridentate ligand with a NNO donor atom system that reacts at very low concentrations with the *fac*-$M(I)(CO)_3^+$ core to form neutral and stable complexes; furthermore, it possesses a second carboxyl group suitable for covalent attachment of a biomolecule bearing an amine group, a process that will render selectivity to the synthesized complexes.[3] In the literature, one method for the attachment of the biologically active molecule on PADA is the prelabeling approach.[6] According to this approach, PADA coordinates to the *fac*-$M(CO)_3^+$ core by the NNO donor atom set leaving the second carboxyl group free and capable of coupling—after activation—to the amine group of the biologically active molecule. A second method[7] for the production of derivatized PADA, involves the use of chloroacetylchloride which on one side reacts with the amine moiety of the biomolecule of interest, while on the other side reacts with the secondary amine of picolylamine monoacetic acid (PAMA) to generate the derivatized PADA.

In this study, we report a convenient method for the synthesis of derivatized PADA ligands through the use of the PADA anhydride (**2**, Scheme 1) which readily couples to free amine functionalities under mild conditions and in high yield. In this first report, aniline, benzylamine, and pyrrolidine were employed as model compounds generating the corresponding ligands **3–5** in high yield (Scheme 1). The synthesis and characterization of the corresponding complexes at carrier level, $^{185/187}$Re(I), and the preparation of the analogous complexes at tracer level, ^{99m}Tc(I), demonstrates the applicability of **2** in the generation of PADA complexes derivatized with primary or secondary amines.

Experimental Section

Synthesis. All reagents and organic solvents used in this study are reagent grade and were used without further purification with the exception of THF which was dried over $LiAlH_4$ and distilled before use. Flash chromatography was performed using Fluca silica gel (60738). Solvents for high-performance liquid chromatography (HPLC) were HPLC-grade. They were filtered through membrane filters (0.22 μm, Millipore, Milford, MA) and degassed by a helium flux before and during use.

IR spectra were recorded as KBr pellets on a Perkin-Elmer 1600 FT-IR spectrophotometer in the region 4000–500 cm^{-1}. The NMR spectra were recorded on a Bruker 500-MHz Avance DRX spectrometer using $(CH_3)_4Si$ as the internal reference. Elemental analyses for C, H and N were conducted on a Perkin-Elmer 2400/II automatic elemental analyzer. HPLC analysis was performed on a Waters 600 chromatography system coupled to both a Waters 2487 Dual λ Absorbance detector and a Gabi gamma detector from Raytest. Separations were achieved on a Nucleosil C18 (10 μm, 250 mm × 4 mm) column eluted with a binary gradient system at a 1 mL min^{-1} flow rate. Mobile phase A was methanol containing 0.1% trifluoroacetic acid, while mobile phase B was water containing 0.1% trifluoroacetic acid. The elution profile was 0 to 1 min

(5) (a) Alberto, R.; Schibli, R.; Waibel, R.; Abram, U.; Schubiger, A. P. *Coord. Chem. Rev.* **1999**, *190–192*, 901–919. (b) Schibli, R.; La Bella, R.; Alberto, R.; Garcia-Garayoa, E.; Ortner, K.; Abram, U.; Schubiger, P. A. *Bioconjugate Chem.* **2000**, *11*, 345–351. (c) Banerjee, S. R.; Levadala, M. K.; Lazarova, N.; Wei, L.; Valliant, J. F.; Stephenson, K. A.; Babich, J. W.; Maresca, K. P.; Zubieta, J. *Inorg. Chem.* **2002**, *41*, 6417–6425. (d) Pietzsch, H.-J.; Gupta, A.; Reisgys, M.; Drews, A.; Seifert, S.; Syhre, R.; Spies, H.; Alberto, R.; Abram, U.; Schubiger, P. A.; Johannsen, B. *Bioconjugate Chem.* **2000**, *11*, 414–424. (e) Kramer, D.; Davison, A.; Davis, W.; Jones, A. G. *Inorg. Chem.* **2002**, *41*, 6181–6183. (f) Müller, C.; Dumas, C.; Hoffmann, U.; Schubiger, P. A.; Schibli, R. J. *Organomet. Chem.* **2004**, *689*, 4712–4721. (g) Dumas, C.; Petrig, J.; Frei, L.; Spingler, B.; Schibli, R. *Bioconjugate Chem.* **2005**, *16*, 421–428. (h) Müller, C.; Schubiger, P. A.; Schibli, R. *Bioconjugate Chem.* **2006**, *17*, 797–806. (i) Saw, M. M.; Kurz, P.; Agorastos, N.; Andy Hor, T. S.; Sundram, X. F.; Yan, K. Y.; Alberto, R. *Inorg. Chim. Acta* **2006**, *359*, 4087–4094. (j) Müller, C.; Hohn, A.; Schubiger, P. A.; Schibli, R. *Eur. J. Nucl. Med. Mol. Imaging* **2006**, *33*, 1007–1016. (k) Spingler, B.; Mundwiler, S.; Ruiz-Sánchez, P.; van Staveren, R. D.; Alberto, R. *Eur. J. Inorg. Chem.* **2007**, 2641–2647.

(6) (a) La Bella, R.; Garcia-Garayoa, E.; Langer, L.; Blauenstein, P.; Beck-Sickinger, A.; Schubiger, P. A. *Nucl. Med. Biol.* **2002**, *41*, 553–560. (b) Langer, L.; La Bella, R.; Garcia-Garayoa, E.; Beck-Sickinger, A. *Bioconjugate Chem.* **2001**, *12*, 1028–1034.

(7) Tzanopoulou, S.; Pirmettis, I. C.; Patsis, G.; Paravatou-Petsotas, M.; Livaniou, E.; Papadopoulos, M.; Pelecanou, M. J. *Med. Chem.* **2006**, *49*, 5408–5410.

100% B, followed by a linear gradient to 30% B in 10 min; this composition was held for another 10 min. After a column wash with 95% A for 5 min, the column was re-equilibrated by applying the initial conditions (100% B) for 15 min prior to the next injection.

Picolylamine *N*,*N*-Diacetic Acid (PADA, 1). PADA was prepared according to published protocols.[8]

4-Pyridin-2-yl-methylmorpholine-2,6-dione (2). A 1 g portion (0.0045 mol) of PADA was dissolved in 20 mL of anhydrous THF with the addition of 1.9 mL (0.0135 mol) of Et_3N. To this solution, 1.15 g (0.0045 mol) of *N*,*N*-bis[2-oxo-3-oxazolidinyl]phosphorodiamidic chloride (BOP-Cl, prepared according to published procedure[9]) was added and the resulting mixture was stirred vigorously under nitrogen in a water bath at 20 °C. After 1 h, the reaction mixture was filtered and the filtrate was used directly for the next step.

Ligands 3–5. The tridentate ligands (phenylcarbamoylmethyl-pyridin-2-ylmethyl-amino)-acetic acid (**3**), [(benzylcarbamoyl-methyl)-pyridin-2-ylmethyl-amino]-acetic acid (**4**), and (2-oxo-2-pyrrolidin-1-yl-ethyl)-pyridin-2-ylmethyl-amino]-acetic acid (**5**) were synthesized according to the same general procedure which is exemplified below for ligand **3**.

(Phenylcarbamoylmethyl-pyridin-2-ylmethylamino)acetic Acid (3). To the solution of the anhydride **2** (0.0045 mol) in 20 mL THF, 0.42 g (0.0045 mol) of aniline were added dissolved in 5 mL of THF. The solution was stirred under nitrogen for 1 h and then evaporated to dryness under reduced pressure. The residue was dissolved in water (5 mL) and extracted with ether (3 × 10 mL). The pH of the aqueous phase was adjusted to 5 with 0.2 M HCl. Subsequently, the aqueous solution was extracted with chloroform (3 × 15 mL). The extract was concentrated and purified by silica gel column chromatography using $CHCl_3$/MeOH (10:2) to give a yellowish solid. Yield: 79%. ^{1}H NMR ($CDCl_3$): δ 8.34 (1H), 7.56 (2H) 7.29 (1H), 7.08 (2H), 6.94–6.81 (3H), 4.74 (NH), 3.59 (2H), 3.33 (2H), 3.01 (2H). ^{13}C NMR ($CDCl_3$): δ176.96, 170.93, 158.17, 149.30, 138.55, 136.53, 128.63, 123.61, 122.17, 119.80, 60.31, 59.39, 58.99.

[(Benzylcarbamoyl-methyl)pyridin-2-yl-methylamino]acetic Acid (4). Yield: 74%. ^{1}H NMR ($CDCl_3$): δ 8.65 (1H), 7.60 (1H), 7.25 (1H), 7.20 (1H), 6.91–6.72 (4H), 3.95 (2H), 3.82 (3H), 3.78 (2H), 3.57 (2H), 3.51 (2H), 3.36 (2H), 2.97 (2H), 2.83 (2H). ^{13}C NMR ($CDCl_3$): δ175.62, 172.21, 157.95, 149.48, 138.31, 137.31, 128.44, 127.62, 127.07, 123.27, 122.69, 60.60, 57.07, 43.27.

[(2-Oxo-2-pyrrolidin-1-yl-ethyl)-pyridin-2-ylmethylamino]acetic Acid (5). Yield: 85%. ^{1}H NMR ($CDCl_3$): δ 8.83 (1H), 7.62 (1H), 7.16 (2H), 4.04 (2H), 3.43 (2H), 3.27 (2H), 3.26 (4H), 1.87 (2H), 1.73 (2H). ^{13}C NMR ($CDCl_3$): δ 175.04, 170.02, 156.60, 150.30, 137.37, 122.83, 122.60, 62.05, 61.82, 58.16, 46.13, 45.84, 25.62, 23.59.

Rhenium Complexes 6–8. The complexes were prepared according to the same general procedure which is exemplified for complex **6**. NMR data for all complexes are given in the NMR section.

$Re(CO)_3$[*o*-$C_5H_4NCH_2N(CH_2CONHC_6H_5)CH_2COO$], 6. To a stirred solution of $[NEt_4]_2[Re(CO)_3Br_3]$ (154 mg, 0.2 mmol, prepared according to published procedure[10]) in 15 mL methanol, ligand **3**(59.8 mg, 0.2 mmol) dissolved in 2 mL methanol was added. The solution was refluxed for 3 h and subsequently the solvent was removed under reduced pressure. The residue was purified by silica gel column chromatography using $CHCl_3$/MeOH (10:2) to give yellowish crystalls. Yield: 75%. IR (cm^{-1}): 2014, 1917, 1884 (*fac*-$Re(CO)_3$). Elemental analysis (%) for $C_{19}H_{16}N_3O_6Re$: C, 40.14; H, 2.84; N, 7.39; found: C, 39.72; H, 2.73; N, 7,26.

Table 1. Summary of Crystal, Intensity Collection, and Refinement Data

	7	**8**
empirical formula	$C_{20}H_{18}N_3O_6Re$	$C_{17}H_{20}BrCa_{0.5}N_3O_7Re$
formula weight	582.57	664.51
temperature	298	298
wavelength	Mo Kα 0.710730	Cu Kα 1.5418
space group	$P2_1/a$	$C222_1$
a (Å)	12.396(4)	22.475(9)
b (Å)	14.440(5)	6.782(2)
c (Å)	12.701(4)	28.418(11)
β (deg)	117.140(10)	
V (Å^3)	2023.1(12)	4332(3)
Z	4	8
D_{calcd} (Mg m^{-3})	1.913	2.038
abs. coeff. μ (mm^{-1})	6.049	14.560
F(000)	1128	2552
goodness-of-fit on F^2	1.068	1.019
R indices	$R1 = 0.0270^a$	$R1 = 0.0541^b$
	$wR2 = 0.0646^a$	$wR2 = 0.1388^b$

[a] For 3066 reflections with $I > 2\sigma(I)$. [b] For 3113 reflections with $I > 2\sigma(I)$.

$Re(CO)_3$[*o*-$C_5H_4NCH_2N(CH_2CONHCH_2C_6H_5)CH_2COO$], 7. Yield: 80 mg (73%). IR (cm^{-1}): 2029, 1931, 1913, (*fac*-$Re(CO)_3$). Elemental analysis calcd (%) for $C_{20}H_{18}N_3O_6Re$: C, 41.23; H, 3.11; N, 7.21; found (%): C, 41.37; H, 3.27; N, 6.86. Crystals suitable for X-ray analysis were obtained by recrystallization from methanol/water.

$Re(CO)_3$[*o*-$C_5H_4CH_2N(CH_2CON(CH_2)_4)CH_2COO$], 8. Yield 58%. IR ($cm^{-1}$): 2030, 1929, 1830 (*fac*-$Re(CO)_3$). Elemental analysis: calcd (%) for $C_{17}H_{18}N_3O_6Re$: C, 37,36; H, 3.32; N, 7.69; found (%): C, 37.61; H, 3.42; N, 7.54. Crystals suitable for X-ray analysis were obtained by recrystallization from methanol/water.

Technetium-99m Complexes 9–11. Technetium-99m complexes, **9**–**11**, were prepared according to the same general procedure which is exemplified for complex **9**: 400 μL of a freshly prepared solution of the *fac*-$[^{99m}Tc(CO)_3(H_2O)_3]^+$ precursor[4] (pH 6) were added to a vial containing a 100 μL solution of **3**(10^{-3} M) in methanol. The vial was flushed with N_2, sealed, and heated for 30 min at 70 °C. HPLC analysis demonstrated the formation of a single complex (radiochemical yield >90%). The radioactivity recovery of the HPLC column after the injection of **9** was monitored and found to be quantitative. The identity of this complex was established by comparative HPLC studies using a sample of the well characterized complex **6** as reference.

X-Ray Crystallography. A colorless crystal of **7** (0.2 × 0.3 × 0.5 mm) was mounted in air on a Crystal Logic Dual Goniometer diffractometer using graphite monochromated Mo Kα radiation. A yellowish crystal of **8** (0.02 × 0.1 × 0.3 mm) was mounted in capillary on a $P2_1$ Nicolet diffractometer upgraded by Crystal Logic using graphite monochromated Cu Kα radiation. Unit cell dimensions were determined by using the angular settings of 25 automatically centered reflections in the range $11 < 2\theta < 23$ ° (for **7**) and $22 < 2\theta < 54$ ° (for **8**) and they appear in Table 1. Intensity data were recorded using a $\theta-2\theta$ scan. Three standard reflections monitored every 97 reflections showed less than 3% variation and no decay. Lorentz, polarization and psi-scan absorption corrections were applied using Crystal Logic software. The

(8) Shepherd, E. R.; Sweetland, A. M.; Junker, E. D. *J. Inorg. Biochem.* **1997**, *65*, 1–14.
(9) (a) Cabre-Castellvi; Palomo-Coll, A.; Palomo-Coll, L. A. *Synthesis* **1981**, 616–620. (b) Diago-Meseguer, J.; Fernandez-Lizarbe, R. J.; Palomo-Coll, A.; Zugaza-Bilbao, A. *Synthesis* **1980**, 547–551.
(10) Alberto, R.; Egli, A.; Abram, U.; Hegetschweiler, K.; Gramlich, V.; Schubiger, P. A. J. *Chem. Soc., Dalton Trans.* **1994**, *19*, 2815–2820.

structures were solved by direct methods using SHELXS-86[11] and refined by full-matrix least-squares techniques on F^2 using SHELXL-97.[12] Further crystallographic details for **7**: $2\theta_{max} = 50$ °, scan speed 4°/min, scan range 1.6 + $\alpha_1\alpha_2$ separation, reflections collected/unique/used 3747/3570 [R_{int} = 0.0140]/3570, 343 parameters refined, $[\Delta\rho]_{max}/[\Delta\rho]_{min}$ = 0.991/−0.732 e/Å^3, $[\Delta/\sigma]_{max}$ = 0.003, $R1/wR2$ (for all data) = 0.0350/0.0688. All hydrogen atoms were located by difference maps and were refined isotropically, all non-H atoms were refined anisotropically. Further crystallographic details for **8**: $2\theta_{max} = 125°$, scan speed 1.5°/min, scan range 2.7 + $\alpha_1\alpha_2$ separation, reflections collected/unique/used 3856/3465 [R_{int} = 0.0455]/3465, 267 parameters refined, $[\Delta\rho]_{max}/[\Delta\rho]_{min}$ = 1.240/−1.205 e/Å^3, $[\Delta/\sigma]_{max}$ = 0.001, $R1/wR2$ (for all data) = 0.0622/0.1473. All hydrogen atoms were introduced at calculated positions as riding on bonded atoms, except those of the water molecule which were not included in the refinement. All non-H atoms were refined anisotropically.

Results and Discussion

Synthesis. Anhydrides of diacids are known to readily react with amine nucleophiles with formation of an amide bond and concomitant release of one free carboxylic acid group. Therefore, reaction of the anhydride of PADA with the amine functionality of a biologically active molecule is expected—in principle—to join the two molecules through an amide bond and at the same time to release the second carboxylic group necessary for the formation of a $M(CO)_3(NNO)$ complex with the $M(CO)_3^+$ core (M = Re, Tc).

A number of attempts to synthesize the PADA anhydride employing various synthetic procedures in the literature proved unsuccessful. For example, reacting the PADA ligand with acetic anhydride[13] a method that requires refluxing, lead to the progressive darkening of the reaction mixture and the generation of black tarry products at only 50 °C. According to another method[14] reported for the formation of diaminetetracetic acid anhydrides, PADA was heated with a monocarboxylic anhydride in the presence of a tertiary amine (pyridine or triethylamine), however, this method led again to tarry undefined products. These results indicated that the PADA anhydride (**2**) is sensitive to heat and prompted us to seek another milder method for its preparation. *N*,*N*′-Dicyclohexylcarbodiimide (DCC) is a mild dehydrating agent frequently employed in the synthesis of carboxylic anhydrides;[15] in the case of PADA, however, it only led to undesired products.

Finally, the method reported by Palomo-Coll for one step synthesis of anhydrides from the tertiary ammonium salts of the carboxylic acids using *N*,*N*-bis[2-oxo-3-oxazolidinyl]phosphorodiamidic chloride[9] (BOP-Cl) was attempted. The main advantages of this method are mild reaction conditions and direct conversion of the appropriate acid to the anhydride. Nevertheless, the instability of **2** toward heating was evident when the solvent was removed at the rotary evaporator at 40 °C. The yellow solution would become dark brown and no anhydride was isolated. As a result it became clear that the anhydride cannot be isolated and its subsequent coupling with an amine functionality should be done in situ. Therefore, after the removal of the solid *N*,*N*-bis[2-oxo-3-oxazolidinyl]phosphorodiamidic acid by filtration, the solution of the PADA anhydride was directly used for the next step. The solution of the anhydride could be used for a period of weeks if kept in the refrigerator.

The reactivity of **2** was tested toward amine nucleophiles by using aniline, benzylamine, and pyrrolidine as model compounds (Scheme 1). The reaction was complete in 1 h under mild conditions at room temperature generating the corresponding adducts **3**–**5** in high yield (75–85%). In each case, only one product was formed as evidenced by HPLC analysis.

The derivatized PADA ligands, **3**–**5** react readily with the $[NEt_4]_2[Re(CO)_3Br_3]$ precursor in methanol to generate the corresponding neutral $Re(CO)_3(NNO)$ complexes **6**–**8** (Scheme 1). After purification by column chromatography, all compounds were collected as yellowish solids and they were characterized by elemental analyses and spectroscopic methods. Crystals suitable for X-ray crystallography were obtained for **7** and **8** by recrystallization from methanolic/aqueous solutions. In the case of **8**, the X-ray analysis revealed the formation of an interesting structure in which four molecules of **8** coordinate with a Ca atom through the oxygens of the amide or the carboxylate carbonyls (see X-ray Crystallography). The presence of the Ca atom in the isolated crystal may either come from the silica gel used during the flash chromatography purification or from the water used in the crystallization procedure.[16]

The infrared spectra of complexes **6**−**8** show strong bands in the 2030–1890 cm^{-1} range, attributed to the C═O stretch of the *fac*-$[Re(CO)_3]^+$ unit.[17] In addition, all complexes exhibit strong broad absorptions in the 1600–1640 cm^{-1} region which correspond to asymmetrical C═O stretching vibration of the coordinated carboxylate and amide groups.

X-ray Crystallography. Compounds **7** and **8** crystallize in the monoclinic space group $P2_1/a$ and in the orthorhombic space group $C222_1$ respectively with one crystallographically independent molecule in the asymmetric unit. The molecular structures of **7** and **8** are given in Figures 1 and 2, respectively, and selected bond distances and angles are listed in Tables 2 and 3. The coordination geometry about rhenium in **7** and **8** is distorted octahedral comprised by the NNO donor atom set of the tridentate ligand and the three carbonyl

(11) Sheldrick, G. M. *SHELXS-86, Structure solving Program*; University of Gottingen: Gottingen, Germany, 1986.
(12) Sheldrick, G. M. *SHELXL-97: Program for Crystal Structure Refinement*; University of Gottingen: Gottingen, Germany, 1997.
(13) (a) Bischoff, C.; Hausdorfer, A. *Chem. Ber.* **1892**, *25*, 2270–2280. (b) Henry, W. D. *J. Heterocycl, Chem.* **1966**, *3*, 503–511. (c) Khilya, V. P.; Lezenko, A. *Zh. Org. Khim.* **1970**, *6*, 2048–2051.
(14) (a) Geigy, J. R. Bis-anhydrides d'acides carboxyliques et leur preparation. Fr Patent 1548888, 1968. (b) Eckelman, W. C.; Karesh, S. M.; Reba, R. C. *J. Pharm. Sci.* **1975**, *64*, 704–706.
(15) (a) Chen, F.; Kuroda, K.; Benoiton, L. *Synthesis* **1978**, *12*, 928–929. (b) Chen, F.; Benoiton, L. *Synthesis* **1979**, *09*, 709–711.
(16) Chi, Y. D.; Wilson, R. S.; Katzenellenbogen, A. J. *Inorg. Chem.* **1995**, *34*, 1624–1625.
(17) (a) Gamelin, D.; George, M.; Glyn, P.; Grevek, F.; Schaffner, K.; Turner, J. *Inorg. Chem.* **1994**, *33*, 3246–3250. (b) Granifo, J. *Polyhedron* **1999**, *18*, 1061–1066. (c) Abel, E.; Ouell, K.; Osborne, A.; Pain, H.; Sik, V.; Hursthouse, M.; Malik, K. *J. Chem, Soc., Dalton Trans* **1994**, 3441–3449. (d) Anderson, P.; Keene, F.; Horn, E.; Tiekink, E. *Appl. Organomet. Chem.* **1990**, *4*, 523–533.

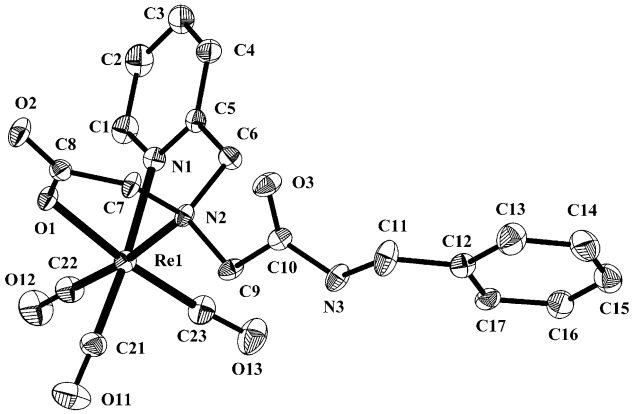

Figure 1. ORTEP plot of the molecular structure of **7** with the atomic labeling (thermal ellipsoids are shown with 40% probability).

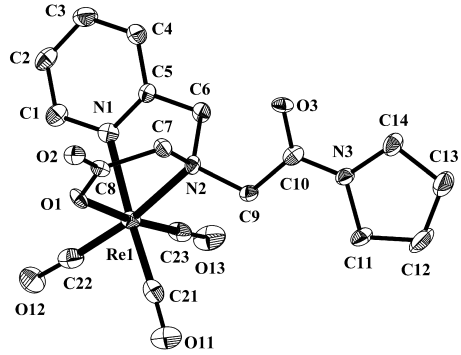

Figure 2. ORTEP plot of the molecular structure of **8** with the atomic labeling (thermal ellipsoids are shown with 40% probability).

Table 2. Selected Bond Distances (Å) and Angles (deg) for **7**

Distances			
Re(1)−C(23)	1.909(6)	Re(1)−O(1)	2.112(3)
Re(1)−C(22)	1.915(6)	Re(1)−N(1)	2.178(4)
Re(1)−C(21)	1.920(6)	Re(1)−N(2)	2.255(4)
Angles			
C(23)−Re(1)−C(22)	88.6(2)	C(21)−Re(1)−N(1)	172.6(2)
C(23)−Re(1)−C(21)	90.6(3)	O(1)−Re(1)−N(1)	79.4(1)
C(22)−Re(1)−C(21)	87.2(3)	C(23)−Re(1)−N(2)	96.1(2)
C(23)−Re(1)−O(1)	173.0(2)	C(22)−Re(1)−N(2)	173.1(2)
C(22)−Re(1)−O(1)	97.1(2)	C(21)−Re(1)−N(2)	97.9(2)
C(21)−Re(1)−O(1)	93.8(2)	O(1)−Re(1)−N(2)	78.0(1)
C(23)−Re(1)−N(1)	95.9(2)	N(1)−Re(1)−N(2)	77.9(2)
C(22)−Re(1)−N(1)	96.5(2)		

groups. The apical positions of the octahedron are occupied by the carboxylate oxygen atom of the tridentate ligand and one of the carbonyl groups. Rhenium lies 0.11 and 0.09 Å above the equatorial plane in **7** and **8** respectively. In **7**, the two five-membered rings in the coordination sphere, defined by the N−C−C−N and the N−C−C−O chelating atoms of the tridentate ligand and the metal ion, adopt the envelope configuration with N2 displaced by 0.50 and 0.36 Å respectively out of the best mean plane of the remaining four atoms. In **8**, the Re−N−C−C−N five-membered ring adopts the envelope configuration with N2 displaced by 0.69 Å out of the best mean plane of the remaining four atoms, while the Re−N−C−C−O five-membered ring is planar. The angles around the metal within the tetragonal plane of the octahedron range from 77.9(2) to 97.9(2)° in **7**, and from 76.5(4) to 97.8(7)° in **8**, whereas those involving the apical

Table 3. Selected Bond Distances (Å) and Angles (deg) for **8**[a]

Distances			
Re(1)−C(21)	1.871(19)	Re(1)−O(1)	2.108(9)
Re(1)−C(22)	1.89(2)	Re(1)−N(1)	2.171(12)
Re(1)−C(23)	1.896(16)	Re(1)−N(2)	2.291(10)
Ca(1)−O(2)	2.308(9)	Ca(1)−O(3″)	2.366(8)
Ca(1)−Ow(1)	2.358(10)		
Angles			
C(21)−Re(1)−C(22)	88.2(7)	C(23)−Re(1)−N(1)	94.3(6)
C(21)−Re(1)−C(23)	89.2(7)	O(1)−Re(1)−N(1)	81.1(4)
C(22)−Re(1)−C(23)	89.5(8)	C(21)−Re(1)−N(2)	97.2(6)
C(21)−Re(1)−O(1)	95.0(5)	C(22)−Re(1)−N(2)	171.5(6)
C(22)−Re(1)−O(1)	94.3(6)	C(23)−Re(1)−N(2)	97.2(6)
C(23)−Re(1)−O(1)	174.4(5)	O(1)−Re(1)−N(2)	78.7(4)
C(21)−Re(1)−N(1)	173.1(6)	N(1)−Re(1)−N(2)	76.5(4)
C(22)−Re(1)−N(1)	97.8(7)		
O(2)−Ca(1)−Ow(1)	90.8(4)	Ow(1′)−Ca(1)−O(3″)	86.8(4)
O(2)−Ca(1)−O(2′)	90.9(5)	Ow(1)−Ca(1)−O(3″)	97.2(4)
O(2)−Ca(1)−O(3″)	83.1(3)	Ow(1)−Ca(1)−O(3‴)	86.8(4)
O(2)−Ca(1)−Ow(1′)	169.9(4)	O(3″)−Ca(1)−O(3‴)	174.3(5)
Ow(1′)−Ca(1)−Ow(1)	89.3(6)	O(2)−Ca(1)−O(3‴)	92.9(3)

[a] Symmetry operations to generate equivalent atoms: (′) = x, 1 − y, −z; (″) = x, 1 + y, z; (‴) = x, −y, −z.

atoms range from 78.0(1) to 97.1(2)° in **7**, and from 78.7(4) to 97.2(6)° in **8**. All bond distances in the coordination sphere fall in the ranges observed in analogous complexes.[4,5]

In the asymmetric unit of **8**, apart from the neutral rhenium complex, there is also a calcium atom sitting on a 2-fold axis of symmetry, a bromide anion and a water molecule The calcium atom is coordinated to two peptide-type oxygen atoms (O3) and two carboxylato oxygen atoms (O2) belonging to four symmetry related rhenium complexes (Figure 3). The octahedral coordination around the calcium atom is completed by two water molecules. The so-formed polymeric structure of **8** extends along the *b*-axis. The bond distances in the coordination sphere of calcium range from 2.308(9) to 2.366(8) Å.

NMR Studies. ^{1}H and ^{13}C chemical shift assignments for complexes **6**–**8** were based on a series of ^{1}H−^{1}H and ^{1}H−^{13}C correlation spectra and are reported in Table 4. The numbering of the atoms is shown in Scheme 1. In all complexes the diastereotopic protons on C-6, C-7, and C-9 appear as three sets of doublets at 5.3–3.6 ppm, as previously observed for similar complexes with the PADA ligand system.[7,18] The sets were distinguished among themselves based on NOE's and long-range heteronuclear couplings. Specifically, protons on C-6 were unambiguously assigned based on the presence of an NOE correlation peak with the H-4 pyridinyl proton. Protons on C-9 are characterized by their long-range coupling to the C-10 carbonyl carbon of the amide group (at approximately 166 ppm in the three complexes and definitely assigned through its coupling to the NH amide proton in complexes **6** and **7**). Finally, protons on C-7 were assigned based on their long-range coupling to the C-8 carbonyl of the coordinated carboxyl group at ca. 179 ppm. The benzylic protons on C-11 of complex **7** appear as an AB system with second-order splitting centered at 4.34 ppm and their long-

(18) (a) Marti, N.; Spingler, B.; Breher, F.; Schibli, R. *Inorg. Chem.* **2005**, *44*, 6082–6091. (b) Wei, L.; Babich, J. W.; Ouellette, W.; Zubieta, J. *Inorg. Chem.* **2006**, *45*, 3057–3066. (c) Stichelberger, A.; Waibel, R.; Dumas, C.; Schubiger, P. A.; Schibli, R. *Nucl. Med. Biol.* **2003**, *30*, 465–470.

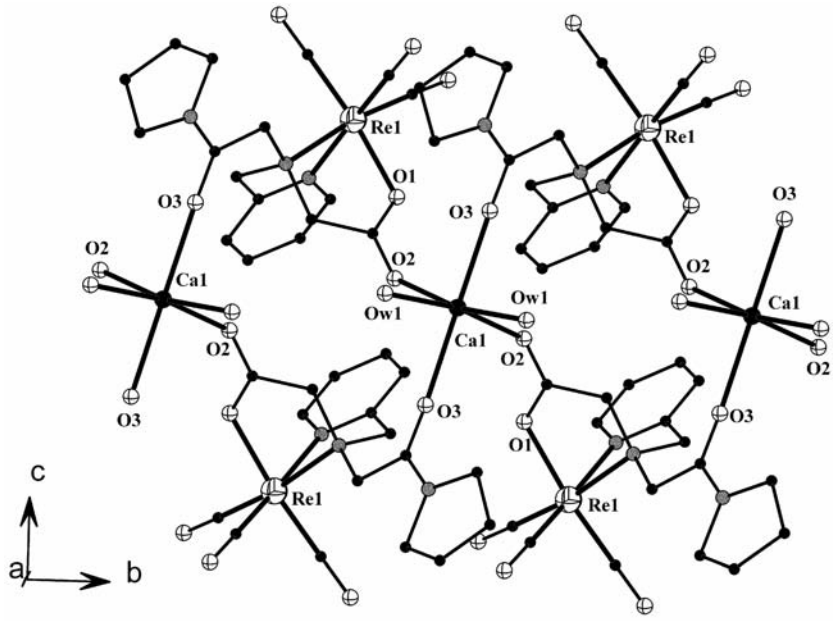

Figure 3. Partially labeled ball and stick plot of the polymeric structure of **8** (color code Re, octant; Ca, large black; C, small black; N, grey; O, white crossed).

Table 4. ^{1}H and ^{13}C NMR Chemical Shifts δ (ppm) for Complexes **6, 7**, and **8** in DMSO-d_6 at 25 °C[a]

	6	7	8		6	7	8
H-1	8.77	8.75	8.75	C-1	151.86	152.02	151.87
H-2	7.59	7.57	7.57	C-2	125.82	125.98	123.94
H-3	8.14	8.12	8.13	C-3	140.51	140.66	140.50
H-4	7.85	7.80	7.82	C-4	124.08	124.19	125.76
H-6	5.23 (A), 4.74 (B) J = 16.3 Hz	5.12 (A) 4.65 (B) J= 16.1 Hz	5.29, (A) 4.66 (B) J = 16.2 Hz	C-5	159.70	159.67	159.82
H-7	4.10 (B) 3.76 (A) J = 17.1 Hz	4.01 (B) 3.64 (A) J = 17.4 Hz	3.96 (B) 3.69 (A) J= 17.4 Hz	C-6	68.15	68.55	68.21
H-9	4.65 (B) 4.10 (A) J= 16.2 Hz	4.45 (B) 4.26 (A) J = 15.6 Hz	4.56 (B) 4.34 (A) J = 16.2 Hz	C-7	61.98	62.05	62.02
H-11		4.34	3.36[b]	C-8	179.03	179.32	179.09
H-12	7.62		1.78[b]	C-9	69.40	68.84	67.75
H-13	7.35	7.33	1.92[b]	C-10	166.51	167.56	165.82
H-14	7.09	7.35	3.40[b]	C-11	138.45	42.26	45.19[b]
H-15	7.35	7.26		C-12	119.23	138.68	23.61[b]
H-16	7.62	7.35		C-13	128.85	127.65	25.71[b]
H-17		7.33		C-14	123.66	128.53	45.65[b]
NH	10.31	8.79		C-15	128.85	127.18	
				C-16		128.53	
				C-17		127.65	
				carbonyls	197.28	197.30	197.31
					196.91	197.02	197.14
							196.95

[a] The atom numbering as well as the designation of the geminal protons on C-6, C-7, and C-9 as A or B is given in Scheme 1. [b] In complex **8**, the assignments of H-11 and H-14 as well as those of H-12 and H-13 may be interchanged; the same holds for the assignments of C-11 and C-14 as well as those of C-12 and C-13.

range couplings were employed in the assignment of the chemical shifts of the aromatic ring (Figure 4).

The stereospecific assignments of the geminal protons on C-6, C-7, and C-9 were based on the combined analysis of NMR and crystallographic data. In all complexes, the intensity of the NOE correlation peaks of the H-4 pyridinyl proton with the two geminal protons on C-6 (A and B in Scheme 1) is differentiated, the one with the most downfield of the two protons being significantly stronger. According to the crystallographic structures of complexes **7** and **8** the distance between proton H-4 and H-6A is on average 2.5 Å while the distance between H-4 and H-6B is 3.1 Å. It is therefore reasonable to assume that the most downfield of the protons on C-6 is the H-6A, and hence differentiate it from H-6B. Using the same argument, the single NOE correlation between protons on C-6 and protons on C-7 (Figure 5) is expected to be one between H-6A and H-7A because the distances recorded in the ORTEP diagrams of **7** and **8** are on the average, H-6A···H-7A 2.3 Å and H6A···H7A 3.2 Å, leading to the stereospecific assignment of protons on C-7. Finally, the correlation of the H-7B and one of the protons on C-9, designates according to the ORTEP distances (average for **7** and **8** H-7B···H-9B 2.2 Å, H-7B···H-9A 3.3 Å) proton H-9B and differentiates it from proton H-9A.

It is interesting to note that in all complexes a ^{4}J coupling is present between protons H-6B and H-7B that exist in a *W* arrangement in the rigid structure of the complexes. The presence of this coupling further confirms the stereospecific assignment of the protons on C-6 and C-7 because in no other spatial placement would these two protons be in a *W* arrangement.

Technetium-99m Chemistry. At technetium-99m level, the complexes *fac*-^{99m}Tc(CO)$_3$(NNO) were obtained almost quantitatively (>90%) by heating the *fac*-[^{99m}Tc(CO)$_3$-(H$_2$O)$_3$]$^+$ precursor at 70 °C in water (pH 6) and in the

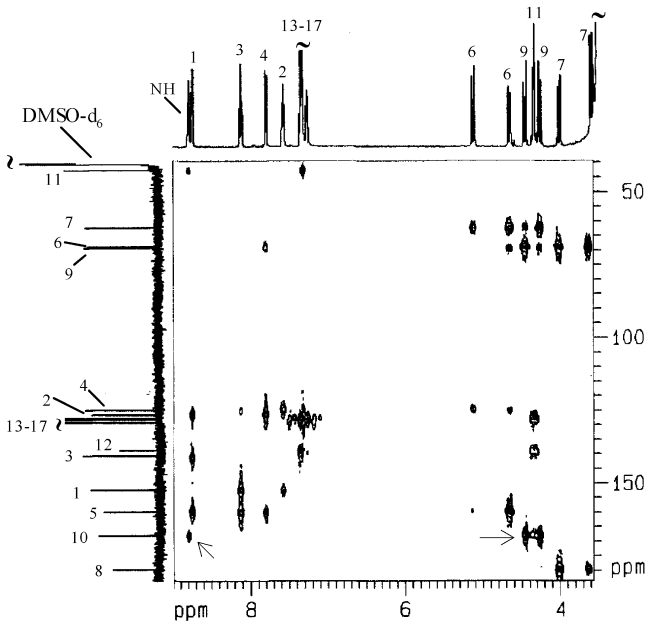

Figure 4. HMBC spectrum (range δH 8.99–3.58, range δC 183.8 – 39.5) of complex **7** in DMSO-d_6 at 25 °C. The arrows show the long-range correlations of C-10 with the amide proton and the two protons on C-9 mentioned in the text.

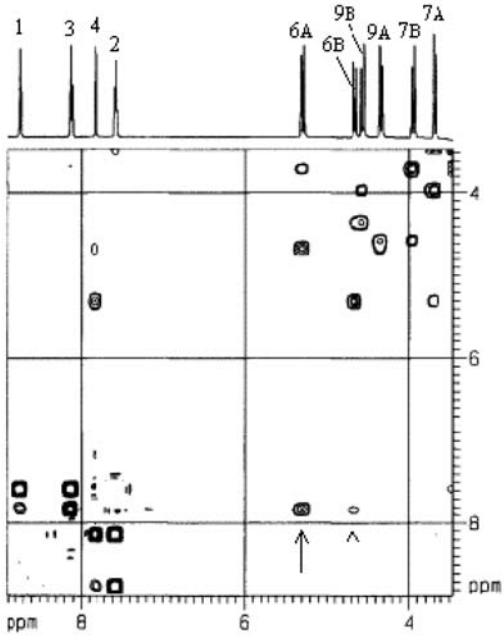

Figure 5. Phase-sensitive NOESY spectrum of complex **8** (range δ_H 8.92–3.46) in DMSO-d_6 at 25 °C. Only the positive peaks are plotted. The arrows show the correlations between the H-4 pyridinyl proton and the geminal protons on C-6.

presence of a 10^{-4} M concentration of the corresponding ligand (**3**–**5**). Their structure was established by HPLC comparison of their retention times to those of the authentic well characterized rhenium complexes by applying parallel radiometric and photometric detection (Figure 6).

In conclusion, a convenient scheme for the preparation of derivatized PADA Re(I) and Tc(I) tricarbonyl complexes is reported. The key feature of the scheme is the use of the anhydride of PADA, **2**, to give in high yield the desired

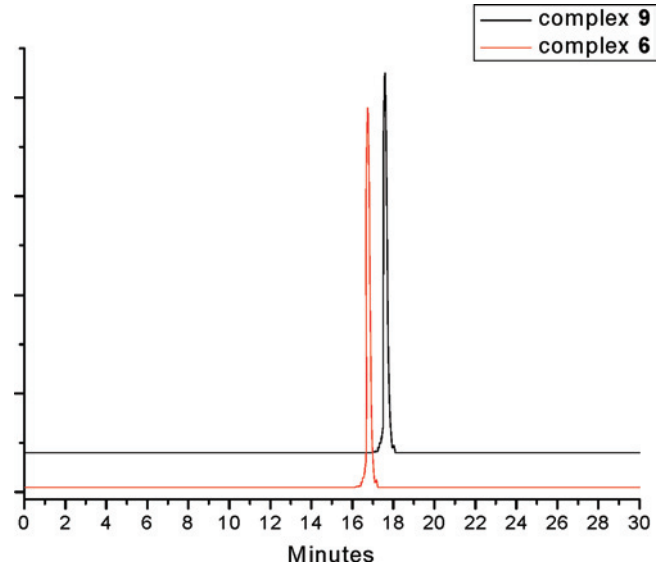

Figure 6. Reverse phase HPLC chromatograms after coinjection of complexes **6** and **9**: (red) UV trace at 254 nm, complex **6**, t_R 16.8 min; (black) gamma trace, complex **9**, t_R 17.3 min.

ligands in a quick, single step under mild conditions. In a broader sense, compound **2** is a bifunctional agent (BCA) because its reaction with an amine nucleophile leads to derivatives carrying a pharmacophore of choise with simultaneous release of the strongly coordinating NNO donor atom set. The proposed scheme was successfully tested by using aniline, benzylamine, and pyrrolidine as model amine nucleophiles, and the corresponding ligands synthesized readily reacted with the $Re(I)(CO)_3^+$ and $Tc(I)(CO)_3^+$ precursors to generate neutral and stable tricarbonyl complexes. Thus, **2** emerges as a versatile starting material for the development of target-specific radiopharmaceuticals for diagnosis and therapy. Already our group has successfully applied this scheme in the synthesis of technetium-99m tricarbonyl complexes with fluoroquinolones[19] for infection imaging, quinazolines[20] for tumor diagnosis and o-methoxyphenylpiperazine for 5-HT_{1A} receptor imaging; the biological evaluation of these complexes is in progress.

Acknowledgment. This work was supported by the General Secretariat of Research and Technology (GSRT) of Greece (PENED01 1081).

Supporting Information Available: Crystallographic data in CIF format for the structures of the complexes **7** and **8**. This material is available free of charge via the Internet at http://pubs.acs.org.

IC7019268

(19) Kyprianidou, P.; Chiotellis, A.; Papagiannopoulou, D.; Tsoukalas, C.; Panagiotopoulou, A.; Pelecanou, M.; Iakovou, I.; Papadopoulos M.; Pirmettis I. In *Technetium, Rhenium and Other Metals in Chemistry and Nuclear Medicine*; Mazzi, U., Ed.; SGEditoriali: Padova, Italy, 2006; Vol. 7, pp 93–4..

(20) Margaritis, N.; Bourkoula, A.; Chiotellis, A.; Papadopoulos A.; Panagiotopoulou, A.; Tsoukalas, C.; Fernades, C. C.; Pelecanou, M.; Paravatou, M.; Livaniou, E.; Santos, I.; Papadopoulos M.; Pirmettis I. In *Technetium, Rhenium and Other Metals in Chemistry and Nuclear Medicine*; Mazzi, U., Ed.; SGEditoriali: Padova, Italy, 2006; Vol. 7, pp 523–524..